

MARCH 1972

# HEWLETT-PACKARD JOURNAL





# Time Domain Reflectometry in Narrowband Systems

By Gene A. Ware

TIME DOMAIN REFLECTOMETRY, or TDR as it is affectionally known, has become well established as a technique for identifying the location and nature of impedance discontinuities in broadband transmission systems. Since reflections from separate discontinuities are spaced apart on the CRT display, the effects of the measuring system may be separated from the system under test, and the location and identity of each of several discontinuities becomes easy—far easier than with CW techniques.<sup>1</sup>

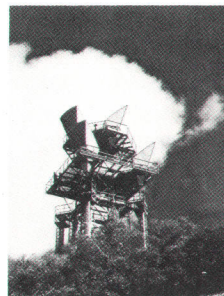
In waveguide and other band-limited systems, though, application of wideband TDR has not been so straightforward.<sup>2</sup> This is because only a small part of the energy in the incident voltage step can enter the system under test while the major part is reflected back to the source. As a result, energy in the reflections may be at too low a level to be detectable, and that which can be detected is of a highly oscillatory form with a long time duration, yielding less than satisfactory time and amplitude resolution in the measurement. This suggests that to be successful, energy in the TDR incident pulse should be confined to a narrow band of frequencies.

Thus, a new TDR system has been developed. This one uses a short burst of RF for the incident pulse, rather than a fast voltage step. Proper selection of the carrier frequency and the burst width confines most of the energy within a frequency spectrum corresponding to the passband of the system under test. This makes it possible to get detectable reflections from small discontinuities—impedance differences as small as 1% being detectable by this system. Hence, the advantages of TDR now become available for use in narrowband systems.

## An Effective Cure

Like its wideband counterpart, the narrowband

system easily resolves multiple discontinuities, a capability that deserves special emphasis. Multiple discontinuities in the antenna feedline of a multi-channel communications system, for example, have much the same effect on system performance that multipath transmissions do, resulting in intermodulation distortion, lower signal-to-noise ratios and, hence, less than maximum system usability. The new narrowband TDR system makes it possible to locate the individual discontinuities, usually resulting from bad connections or corrosion, cracks,



**Cover:** Keeping a microwave communications repeater—like the one shown on the front cover—operating at full efficiency means that the waveguide feedlines must be free of impedance discontinuities. Particularly disconcerting are multiple discontinuities, which degrade system performance

in much the same way that multipath transmissions do. Described in this first article is an instrument that tells in just a few minutes when more than one discontinuity exists, and where to look for them. This means that cleaner performance can be obtained in less time.

## In this Issue:

*Time Domain Reflectometry in Narrowband Systems*, by Gene A. Ware ..... **page 2**

*Measuring High-Value Capacitors*, by Yoshihisa Kameoka..... **page 8**

*Measuring True RMS AC Voltages to 100 MHz*, by J. B. Folsom ..... **page 14**



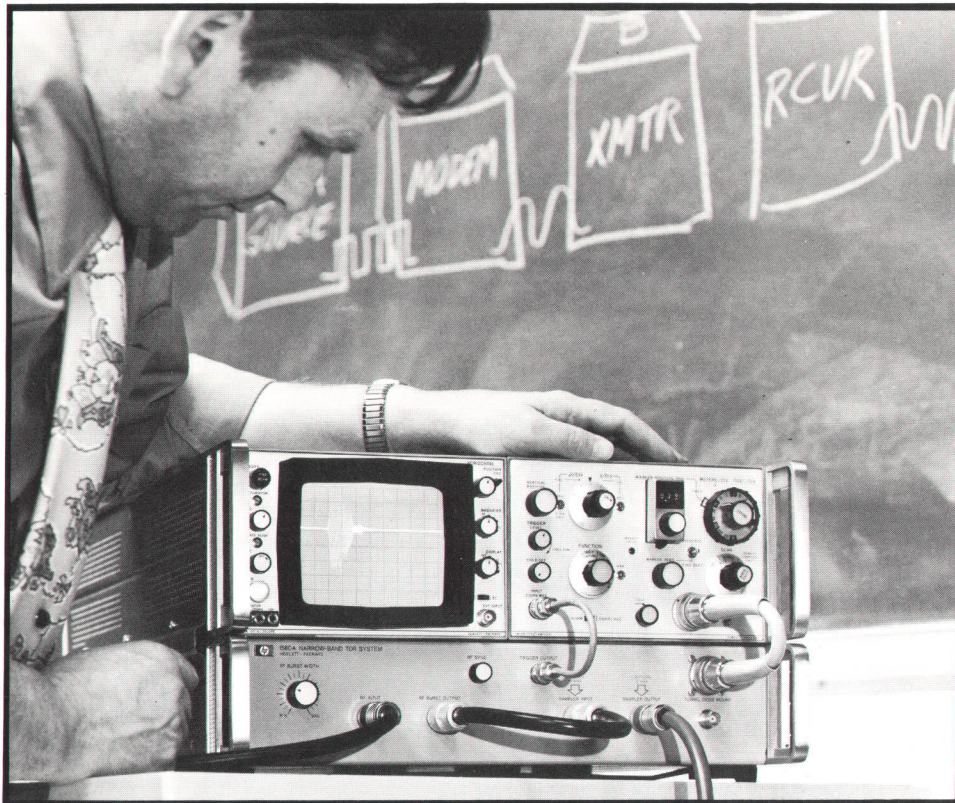


**Fig. 1.** Impedance discontinuities in waveguide and narrowband coaxial transmission systems are easily located with Model 1580A Narrowband Time Domain Reflectometer System. Microwave signal source (not shown) supplies energy for RF bursts. System can also be used for wideband applications with optional tunnel diode voltage step generator.

or foreign objects in the waveguide, so that the system can be 'cleaned up' very quickly to achieve full use of all channels in the communications system.

#### Contraindications

Because the bandwidth of the incident signal is limited, however, this system does not have the resolution capability of the wideband systems. The closest spacing between discontinuities that can be resolved in waveguide is about a foot or so depending on the waveguide and discontinuity location. Also, since it is necessary to examine the phase of the RF carrier to find the nature of a discontinuity (inductive, capacitive, or purely resistive), the system does not easily provide positive identification of the kind of discontinuities encountered. Nevertheless, the system provides information about the magnitude and position of discontinuities quickly and clearly; it is especially useful where multiple discontinuities are involved.

#### Applications in waveguide

To make most effective use of this system in checking out the performance of a waveguide system, certain characteristics of waveguide must be borne in mind. Just about all of the electrical parameters of waveguide are frequency dependent,

usually in a non-linear fashion. The frequency dependence of propagation velocity, or group velocity, is one that can have a pronounced effect on TDR measurements.

Propagation velocity, shown in Fig. 2, is zero at the waveguide's cutoff frequency but rises rapidly as the frequency increases, approaching the speed of light. This can cause dispersion spreading of RF bursts since the frequency components travel at differing velocities. Obviously, pulse dispersion spreading increases with waveguide length, but in addition to that, dispersion spreading is inversely related to burst width (the narrower the burst, the wider the frequency spectrum). The effect is most pronounced for energy at frequencies near the waveguide cutoff frequency.

Ordinarily, resolution is increased as the incident RF burst is narrowed but in the case of waveguide, resolution may suffer from dispersion distortion when the burst is made too narrow. There exists, then, an optimum burst width for any measurement situation. This can be found for a given carrier frequency by varying the width of the incident RF burst while observing the echo returned from a short or other discontinuity at the end of the waveguide run. The optimum incident width is that which gives the minimum echo width. Fig. 3 shows approximate pulse widths in RG52 and RG48



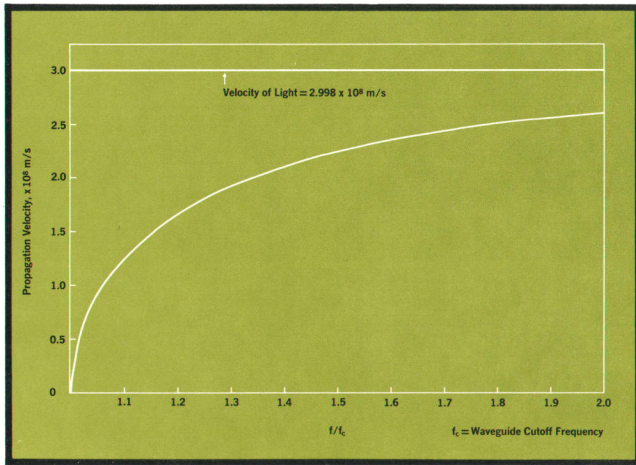


Fig. 2. Velocity of propagation in waveguide as a function of relative frequency.

for different pulsed carrier frequencies. For example, the optimum width at 11 GHz is about 6 ns for 300 feet of RG52.

At 11 GHz, propagation velocity is 1.23 ft/ns in RG52, so on the TDR display a 6-ns burst occupies the equivalent of about 7 feet. Two discontinuities spaced somewhat closer than this could be distinguished but care must be exercised in physically locating the discontinuities because interference between the carriers of the two returns may cause the peaks on the resulting display to show the discontinuities as spaced further apart.

If measurement parameters allow a choice in carrier frequency (normally the carrier is set to the frequency that is expected to be used during normal operation of the waveguide), better resolution is obtained by setting the carrier towards the upper end of the guide's passband. This is because the propagation velocity changes less steeply as a function of frequency at the upper end of the passband than it does at the lower end, resulting in less pulse dispersion (see Fig. 2).

Varying the frequency while watching for changes in the magnitude of a reflection, incidentally, is a means of determining whether a discontinuity is inductive or capacitive. In addition, sweeping of the carrier frequency will aid in the location of highly resonant discontinuities.

#### Applications in coaxial cable

The narrowband TDR system also has applications in coaxial cable, the traditional domain of wideband TDR's. Most important is its use in communications system where filters may interfere with wideband TDR operation. The narrowband TDR system can 'look through' the filters to exam-

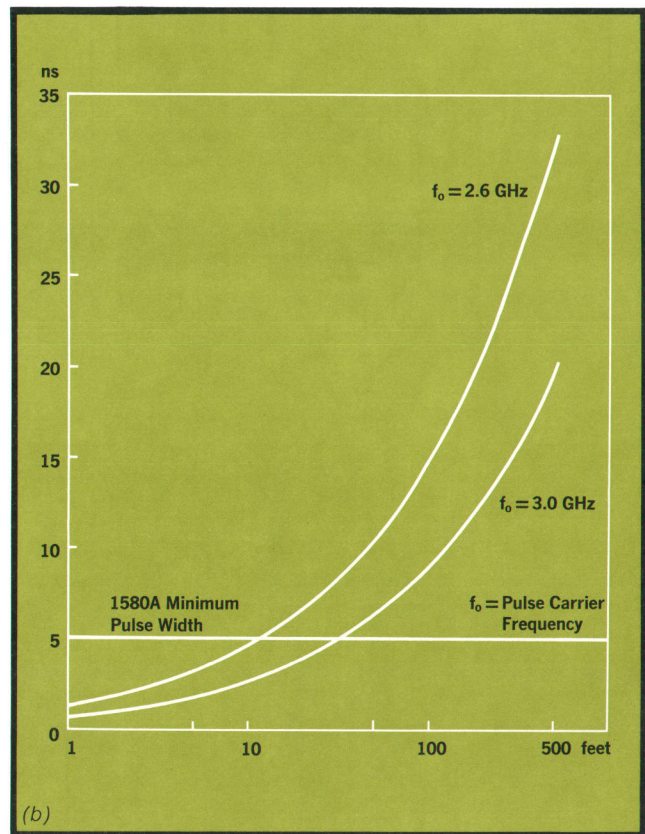
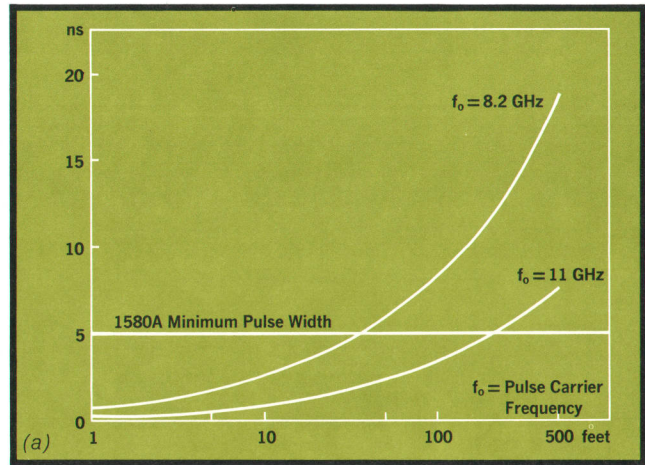


Fig. 3. Approximate optimum pulse width vs guide length in X-band waveguide RG-52 (a), and in S-band waveguide, RG-48 (b).

ine characteristics of the transmission system beyond.

In such an application, it should be remembered that the pulse width will be inversely proportional to the filter bandwidth. This can cause a reduction in resolution. If the burst width is increased to the point that reflections are superimposed on the excitation waveform, these reflections will add



algebraically to the incident waveform. As in the case of overlapping multiple discontinuities, the nature of the waveform depends on the relative phase of the carriers in the incident and reflected signals. The waveform is thus affected by the location as well as the nature of the discontinuities. In this case, quantitative information about the magnitude of the discontinuity is difficult to obtain.

Another application is in finding narrowband discontinuities in a wideband transmission system. The RF burst carrier can be tuned or swept to find these discontinuities. A good example is the identification of low-level, periodic discontinuities resulting from regularly recurring variations in the mechanical structure of coaxial cable (a cable with a center conductor support formed in a helix, for example). By using an RF burst wide enough to span a large number of these discontinuities, the individual discontinuities—normally too small to be detected by wideband techniques—integrate up to form a large discontinuity at a carrier frequency determined by the periodicity of the discontinuities. To determine this 'suck-out' frequency, the pulse carrier frequency is varied until such a discontinuity appears. The discontinuity spacing can then be determined from the carrier frequency and the magnitude of the individual discontinuities can be determined from the rising portion of the reflection.

### The System

The Model 1580A Narrowband TDR System consists of a 180D Oscilloscope with a modified 1815A TDR plug-in and a new RF gating unit (the 1815A TDR plug-in is modified to allow triggering on sine waves when in the TDR mode of operation).

A block diagram is shown in Fig. 4. An external microwave source feeds a PIN-diode switch and a trigger countdown unit. The trigger countdown output is fed into the trigger circuitry of the 1815A TDR plug-in which in turn triggers the pulse generator that controls the PIN-diode switch. This arrangement allows the user to synchronize the gating pulse with the RF carrier, making possible the use of the signal-averaging circuit of the TDR plug-in to improve the signal-to-noise ratio.

The PIN-diode switch is normally off. In this condition, the PIN diodes are biased on, shorting the RF source to prevent any signal transfer to the output port.

The pulse generator turns on the PIN-diode switch (diodes biased off) to produce a burst of RF. The width of the burst is controlled by the pulse generator and may be varied from less than 5 ns to more than 100 ns. The system generates an RF burst with a risetime of less than 1.5 ns. The burst is somewhat Gaussian in shape for burst widths of a few nanoseconds but it becomes rectangular for longer bursts. A typical burst is shown in Fig. 5.

The RF burst is passed through a broadband isolator that removes low-frequency transients generated by the switching of the PIN-diode switch. The isolator also provides a good (1.5:1 VSWR) output impedance match. This is necessary since the PIN-diode switch presents a short circuit at its output when off. The pulse is then passed through a jumper to the 1817A Sampling Head and then into the system under test (the jumper cable can be removed to allow transmission measurements).

The PIN-diode switch can gate RF carriers in a

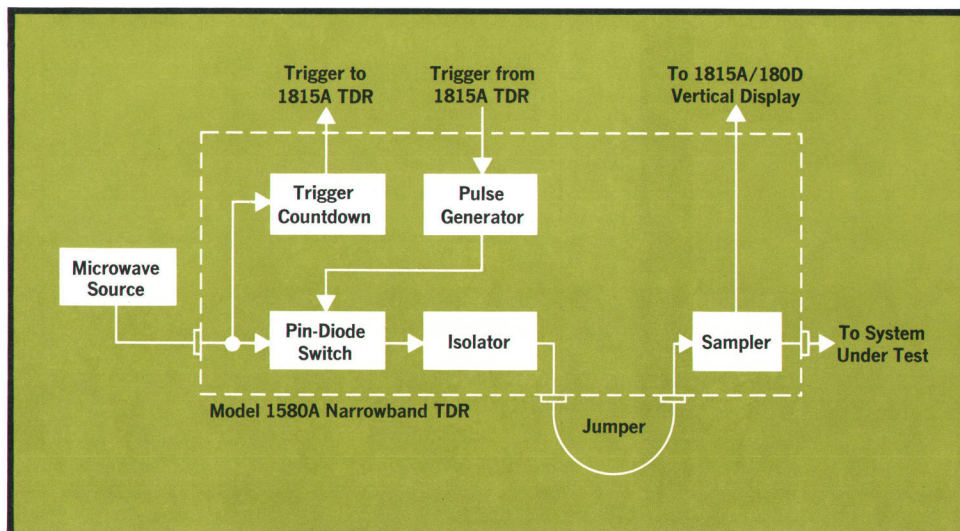
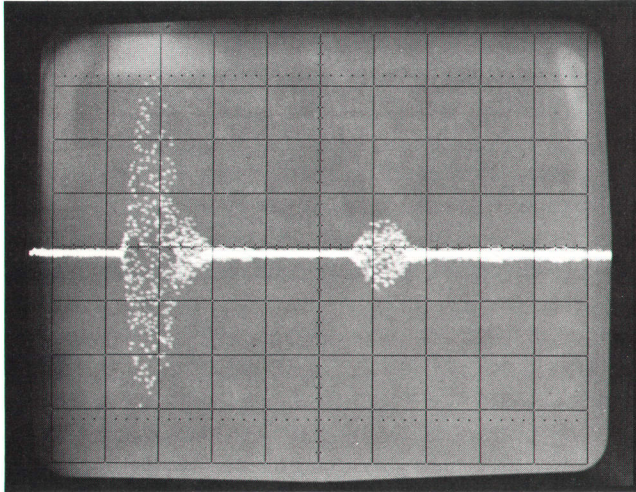


Fig. 4. Block diagram of RF gating unit in Narrowband TDR system.





**Fig. 5.** Typical narrowband TDR display showing interrogating 10-ns burst of 6-GHz carrier and 20% reflection from impedance discontinuity. Horizontal scale factor of 10 ft/div establishes distance to discontinuity as 44 feet.

range from 1 GHz through 12.4 GHz, and on up to 18 GHz with some reduction in specifications. The isolator normally supplied with the system operates from 3.5 GHz to 12.4 GHz. Other frequency ranges may be obtained by using other isolators, optionally available.

The vertical scale of the TDR display is calibrated in units of reflection coefficient by adjusting the incident RF burst to the 'one' level on the display. The magnitude of a reflection (reflection coefficient) may then be read directly from the display, but it must be corrected for guide losses. The loss per foot of guide is usually available but if not, guide losses may be determined by placing a short at the point where the discontinuity occurs. Alternatively, the display may be calibrated with the reflection from the short.

The correction for waveguide losses is best handled by converting the reflection coefficient into return loss. The HP Reflectometer Calculator or a nomograph such as the one in Fig. 6 may be used for the conversion. The return loss can then be

corrected by subtracting the round trip waveguide losses.

Dispersion, if present, can affect the calibration. Normally, dispersion effects are eliminated by lengthening the RF burst, but if this is not practical, then the effects of dispersion may be normalized by using a short at the point of discontinuity.


#### Dynamic Range

Several factors affect the size of the smallest observable return on the Model 1580A NBTDR System. One factor is the noise in the 1815A/1817A TDR plug-in/sampler combination (<8 mV). A second is leakage through the PIN-diode switch. Normally, the on/off ratio of the switch is greater than 40 dB. This provides 40 dB of dynamic range if the incident pulse is at least 40 dB above the noise of the sampler. Higher RF levels, limited to +20 dBm by the PIN diode switch feedthrough and the maximum signal level acceptable to the 1817A Sampler (2 V peak-to-peak), can give somewhat greater dynamic range.

The dynamic range is also interrelated with the maximum usable distance range. Although the display can read up to 10,000 feet, waveguide losses, typically 8.64–6.02 dB/100 ft in X band, limit the maximum range at which any discontinuity can be discerned. The maximum range also depends on the magnitude of the continuity.

Provision has been made to allow use of the 1815A TDR plug-in as a conventional TDR for wideband applications. This usage requires the addition of either the Model 1106A (20 ps) or 1108 (60 ps) tunnel-diode mounts for generating voltage steps.

#### Acknowledgments

Electrical design of the Model 1580A Narrowband TDR was performed by Thomas Edwards and mechanical design by James Arnold. Many helpful ideas were contributed by Jeffrey Smith, William Farnbach, and James Johnson. 

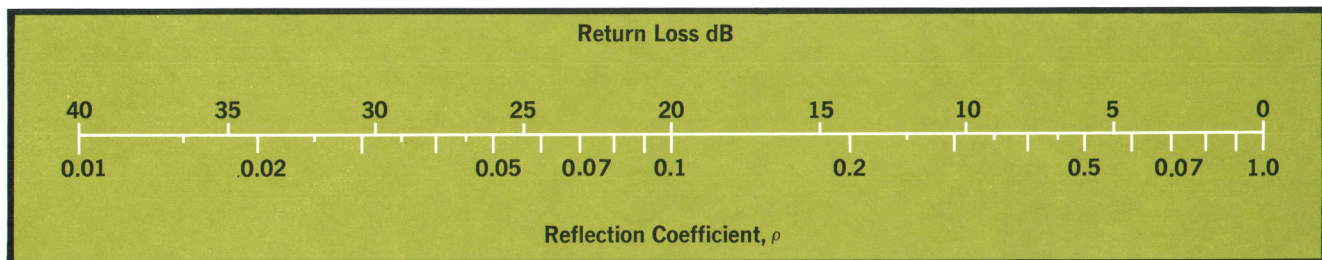


**Fig. 6.** Nomograph converts reflection coefficient into return loss.



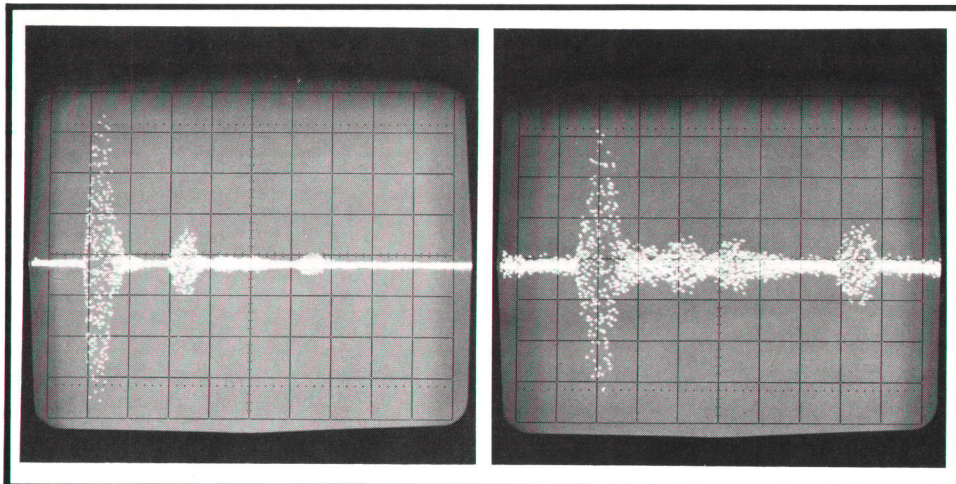
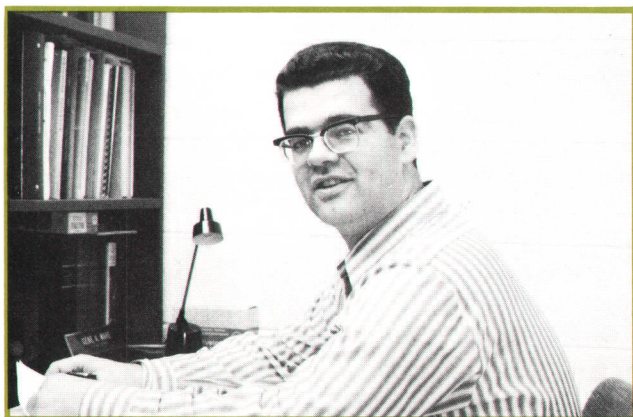


**Fig. 7.** Multiple discontinuities are separated on display for easy identification. Photo at far left, with horizontal scale of 10 ft/div, clearly shows discontinuities at 22 feet and 54 feet and it indicates possibility of discontinuities at 32 and 40 feet. Expanding horizontal scale 2 times and vertical scale 5 times (photo near left) shows that these suspected discontinuities do exist, that they have a reflection coefficient of 0.03, and that they are 7 feet apart.

## References

1. Bernard M. Oliver, 'Time Domain Reflectometry,' Hewlett-Packard Journal, February 1964.
2. Gene A. Ware, 'Narrowband Time Domain Reflectometry,' The Microwave Journal, June 1971.



### Gene A. Ware

Gene Ware first worked for HP's Colorado Springs Division in the summer of 1965 between the time he earned his BSEE degree at Brigham Young University and the time he started on an MSEE degree at the same institution. He came to HP full-time a year later, going to work on the Narrowband TDR (by some strange coincidence, his Master's thesis was on Waveguide Time-Domain Reflectometry). Gene had started his academic career at University of Utah but left after two years to do a four-year hitch in the Army as a Nike Ajax fire-control technician.

Gene again returned to the academic fold a year ago, this time working towards a PhD in biomedical engineering at Utah State University. That activity, plus raising six kids ranging from 4 months to 10 years, doesn't leave any time for flying, an activity he once enjoyed. He does manage to slip away, though, for a little fishing now and then.

## SPECIFICATIONS

### HP Model 1580A Narrowband TDR

#### SYSTEM

**FREQUENCY:** 3.5 GHz to 12.4 GHz. Measurements may be extended to 1 GHz and 18 GHz with reduced performance.

**AMPLITUDE RESOLUTION:** >40 dB (with 70 mW signal source) equivalent to reflection coefficient of 1%.

**SPURIOUS RESPONSE:** Time for spurious responses to settle to within 5% or less of incident burst amplitude is less than 10 ns after end of incident burst.

#### BURST GENERATOR

**INSERTION LOSS:** Nominally 10 dB

**RISETIME:** Nominally 1.5 ns

**ON/OFF RATIO:** >40 dB.

**PULSE BURST WIDTH:** <5 ns to >100 ns.

#### SAMPLER

**BANDWIDTH:** dc to 12.4 GHz, 3 dB down at 12.4 GHz.

**INPUT DYNAMIC RANGE:** 2 V p-p.

**MAXIMUM SAFE INPUT:**  $\pm 3$  V.

**NOISE:** 8 mV.

#### OSCILLOSCOPE

Standard 5¼-inch high rack-model oscilloscope, refer to 180 system data sheet for specifications. Mainframe can also be used with 1800 series plug-ins for general purpose troubleshooting and design.

#### TDR/SAMPLER PLUG-IN

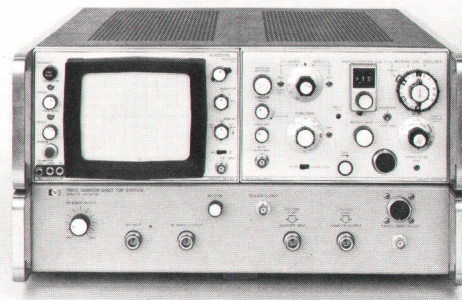
1815A/B plug-in modified (option 001) to accept external triggering in TDR mode. Refer to 1815A/B data sheet for complete specifications. Model 1815A is calibrated in ft/div and 1815B is calibrated in meter/div.

#### GENERAL

**WEIGHT:** Net, 44 lb (20 kg); shipping, 59 lb. (26.8 kg).

**DIMENSIONS:** 19 in wide x 8¾ in high x 21¾ in deep (483 x 222 x 543 mm).

**PRICE IN U.S.A.:** Model 1580A/B Narrowband TDR (with 180D Oscilloscope and 1815A/B TDR plug-in) **\$6000.**





# Measuring High-value Capacitors

By Yoshihisa Kameoka

*High-capacitance electrolytics have been difficult to measure. New circuit developments make 'touch and read' measurements possible.*

HIGH-VALUE ELECTROLYTIC CAPACITORS are used in very large quantities in all types of electronic equipment, including computers, consumer products and in many industrial applications. Capacitor values up to 0.1 farad (100,000  $\mu\text{F}$ ) are quite common in low-voltage power supplies. Measurements of these high-value electrolytics are difficult because of their low impedance, high dissipation factor and limited voltage rating. A dc bias is also required during measurement. Until recently, there have been no convenient measuring methods.

Electrolytic capacitors can degrade in storage, so in many cases it is necessary to verify their characteristics before use. Also, they slowly degrade in use in power supply circuits. For the manufacturer and user of such capacitors, two new Hewlett-Packard instruments, the HP Model 4350A and 4350B High Capacitance Meters, Fig. 1, have been designed. These instruments simultaneously measure capacitance and dissipation factor ( $\tan \delta$ ). The Model 4350A also measures capacitor leakage current. They are 'touch and read' instruments, not bridges, so they are convenient to operate. Measured values are immediately displayed on front-panel meters, so measurement is quick.

Twelve ranges cover from 1  $\mu\text{F}$  to 300 millifarads. Resolution can be as good as 0.02  $\mu\text{F}$ . Basic accuracy of capacitance measurement is 2% to 4% depending upon range. Dissipation factor ( $\tan \delta$ ) is measurable from 0.05 to 5 in two ranges. The internal test frequency is 120 Hz, which is the fundamental of the ripple frequency of a full-wave power supply. (For electrolytic capacitors a 120-Hz test frequency is generally standard; there are special exceptions.)

The test voltage across the capacitor under test

is usually between 0.5 mV rms and 2.5 V rms, depending upon dissipation factor. An internal dc bias from 0 to 6 volts is available to superpose the ac test signal upon a dc bias voltage. This satisfies a MIL specification for testing tantalum electrolytic capacitors. The Model 4350A measures leakage currents from 0.02  $\mu\text{A}$  to 10 mA in nine ranges. Accuracy is  $\pm 3\%$  of full scale. Internal dc bias voltages up to 100 volts, for leakage current measurement, are available. Up to 600 volts dc bias may be connected to the sample through the instrument, using an external dc voltage source. Leakage current and the dc bias voltage are indicated simultaneously on the front-panel meter.

## Four-Terminal Measurements

To measure devices of very low impedance with high accuracy, the four-terminal method is useful to eliminate errors due to contact resistance and test lead impedance. For example, the reactance of a 300-millifarad capacitor is only 4.4 milliohms at 120 Hz. Often the impedance of contacts and test leads is 30 milliohms or more.

A general four-terminal measurement circuit is shown in Fig. 3. Two of the four terminals are *current* terminals; the others are *potential* terminals. The current terminals supply constant current to the unknown sample, and the potential terminals detect the voltage drop across the sample. In Fig. 3,  $R_s$  is the range resistor; its value is set much larger than  $Z_x$ , the current test lead impedance  $Z_i$  and the contact resistance  $r_i$ . Therefore, the current  $i$  is affected very little by them. Thus, the effect of  $Z_i$  and  $r_i$  in the current terminals loop can be neglected.

The potential terminals are connected only to the two sides of the unknown, so we measure only the





**Fig. 1.** Two new instruments for measurement of high-value capacitors: Hewlett-Packard Model 4350A (left) and 4350B (right). The Model 4350A reads capacitor leakage current in addition to capacitance.

voltage drop,  $e_x$ , across  $Z_x$ . Since the input impedance of the voltmeter is very large we can neglect both the impedance,  $Z_v$ , and the contact resistance,  $r_v$ , of the potential test leads.

Another type of error that can occur in high capacitance measurements is the result of mutual inductance between the current leads and the potential leads. Fig. 4 shows this as a transformer effect; the measured capacitance value is increased

or decreased depending upon the direction of coupling. This error is effectively eliminated if either the current leads or potential leads are twisted to reduce the mutual inductance.

### Capacitance Measurements

Generally, a capacitor is represented by a series equivalent circuit. Capacitance in a series equivalent circuit is usually measured using the voltage-

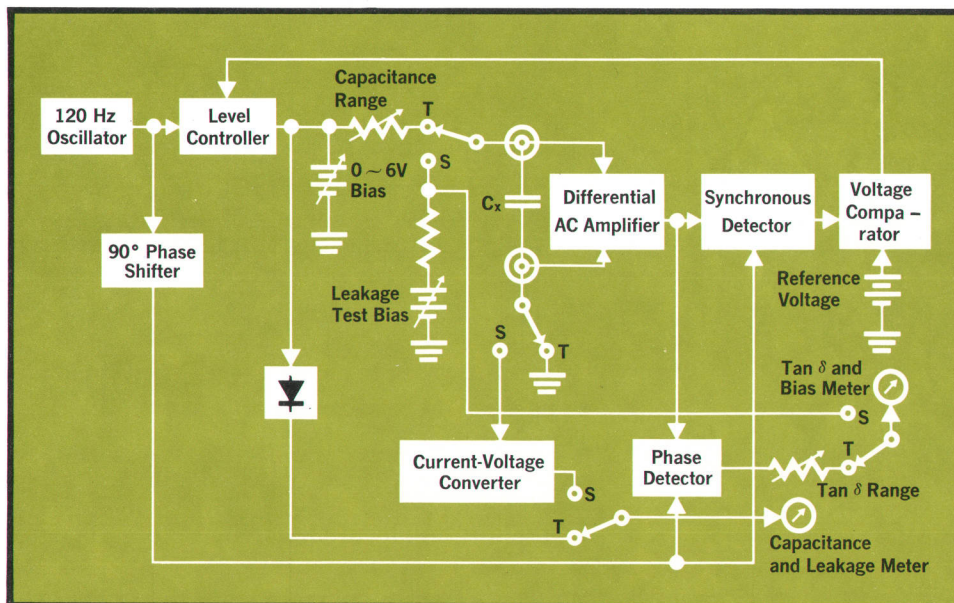


**Fig. 2.** In this block diagram of the Model 4350A, switch position T is for capacitance and  $\tan \delta$  measurement; switch position S is for leakage measurement and bias voltage setting.



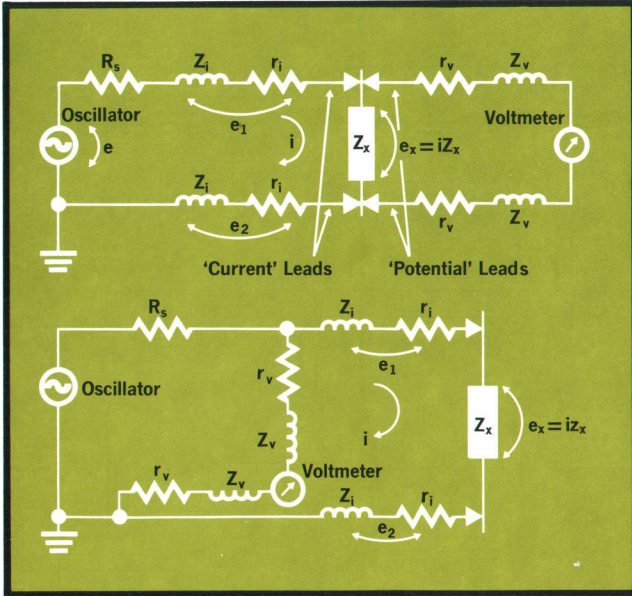


Fig. 3. Equivalent diagram of the four-terminal method of measurement (top) compared to a simple two-terminal method (bottom).

current method, Fig. 5. A 120-Hz oscillator supplies a test signal to the unknown sample, and the voltage drop across the unknown is amplified and measured.

In Fig. 5 the range resistor,  $R_s$ , is much larger than the unknown impedance,  $Z_x$ , so the current flowing through the unknown sample depends only upon the selected range resistor,  $R_s$ , and the output voltage of the 120-Hz oscillator. The ac differential amplifier amplifies the voltage drop across the unknown sample, and supplies it to the synchronous detector.

The amplified voltage drop is fed to one input

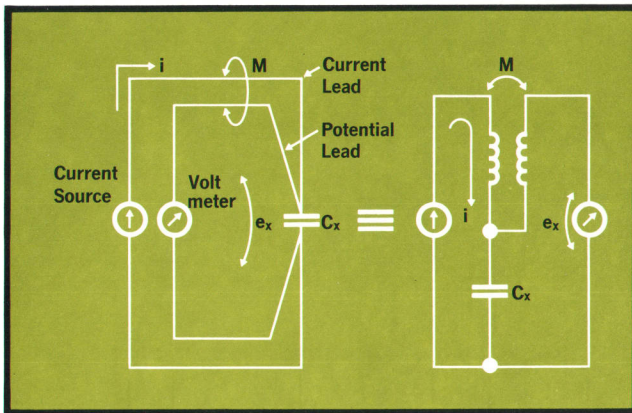


Fig. 4. Mutual inductance between current and voltage leads can result in errors in capacitance measurement.

$$e_x = \left( \frac{1}{j\omega C_x} + j\omega M \right) i, \text{ or } \left( \frac{1}{j\omega C_x} - j\omega M \right) i.$$

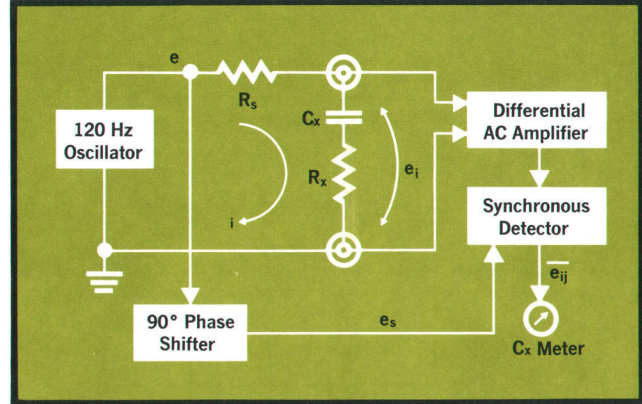


Fig. 5. Voltage-current method commonly used for capacitance measurements.

terminal of the synchronous detector, and the square-wave reference signal is connected to the other. So the output of the detector is a dc voltage proportional to that component of the amplified voltage drop that is in phase with the reference square-wave signal. A 90-degree phase shifter supplies the reference square-wave to the synchronous detector, and this square-wave lags the measuring 120-Hz signal by 90 degrees. It can be shown mathematically that the output to the meter is not linear; this creates calibration difficulties.

Linear output is obtained with the new capacitance measuring circuit, Fig. 6, used in the Model 4350A/B. The level controller has ac input and output terminals, plus a dc input terminal which is used for gain control. AC gain of this level controller is varied by the dc input signal. Then the voltage drop  $e_i$  across the unknown sample is

$$e_i = \frac{R_x + \frac{1}{j\omega C_x}}{R_s + R_x + \frac{1}{j\omega C_x}} e_m \quad (1)$$

where  $e_m$  = output voltage of the level controller.

In the Model 4350A/B the range resistor,  $R_s$ , is about one thousand times larger than the impedance of the unknown sample at full scale. Therefore

$$e_i \cong \left( \frac{R_x}{R_s} + \frac{1}{j\omega C_x R_s} \right) e_m \quad (2)$$

The output dc voltage of the synchronous detector is

$$\overline{e_{ij}} = \frac{K_1 e_m}{\omega C_x R_s} \quad (3)$$

where  $K_1$  is the gain of the synchronous detector and ac amplifier (a constant).

This dc voltage is compared to the constant dc



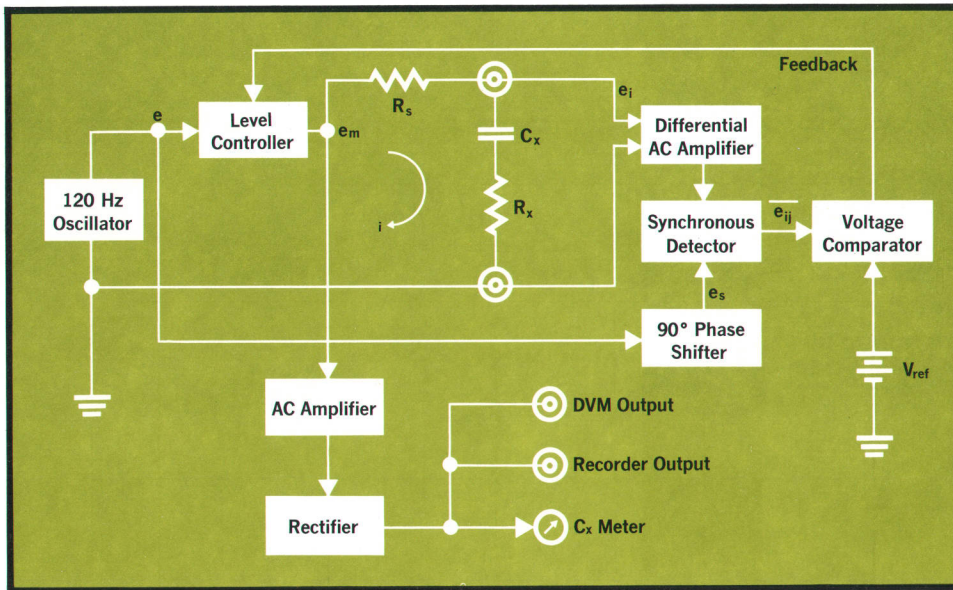


Fig. 6. Linear output to the  $C_x$  meter is obtained with this new measuring circuit used in the Models 4350A/B.

voltage  $V_{ref}$  at the comparator. When  $e_{ij}$  is lower than  $V_{ref}$ , the output voltage of the comparator is proportional to the difference, and is fed back inversely to the control input terminal of the level controller. Hence its ac gain is increased.

Conversely, when  $e_{ij}$  is higher than  $V_{ref}$ , the ac output of the level controller is decreased. Therefore, the feedback circuit of Fig. 6 controls  $e_{ij}$  so as to make it equal to  $V_{ref}$  in spite of the unknown sample value. These relations are expressed by the following equations:

$$\overline{e_{ij}} = \frac{K_1 e_m}{\omega C_x R_s} = V_{ref} = \text{constant} \quad (4)$$

$$\text{Or,} \quad C_x = \frac{K_1 e_m}{\omega R_s V_{ref}} \quad (5)$$

Since  $R_s$  and  $\omega$  are constant,

$$C_x = K_2 \cdot e_m \quad (6)$$

where  $K_2 = K_1 / \omega R_s V_{ref} = \text{constant}$

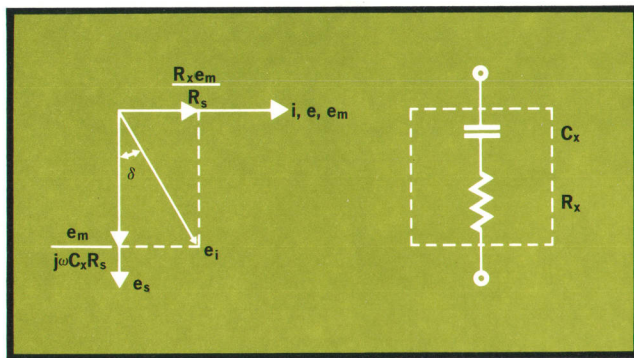


Fig. 7. Vector diagram showing phase relationships in Fig. 6.

Equation (6) shows that the capacitance of the unknown sample is proportional to the output voltage of the level controller. Thus the capacitance of the unknown sample can be read directly on the ac voltmeter, which has a capacitance-calibrated linear scale.

#### Dissipation Factor ( $\tan \delta$ ) Measurements

Electrolytic capacitors have some loss resistance in series with their capacitance. The dissipation factor of the capacitor is defined in a series equivalent circuit as follows:

$$\text{Dissipation Factor} = j\omega C_x R_x \quad (7)$$

where  $R_x =$  equivalent series resistance of capacitor

$C_x =$  capacitance

Fig. 7 is a vector diagram showing the phase relations of each voltage or current of Fig. 6. Phase difference  $\delta$  is called a loss angle. In Fig. 7,

$$\tan \delta = \frac{R_x e_m / R_s}{e_m / j\omega C_x R_s} = j\omega C_x R_x \quad (8)$$

Therefore, the dissipation factor of the capacitor can be represented as the tangent of the phase difference  $\delta$ . Thus if we measure the phase difference between  $e_s$  and  $e_i$  we can determine the dissipation factor of the unknown capacitor.

Fig. 8 is a simplified block diagram for the dissipation factor measurements. The phase detector has two input terminals and one output terminal. Output voltage of this detector is a dc voltage proportional to the phase difference between the two signals at its input. This output voltage is amplified and displayed on the  $\tan \delta$  calibrated meter.



### Leakage Current Measurements

The simplified block diagram of the leakage current measuring scheme (Model 4350A only) is shown in Fig. 9.  $V$  is the dc source that supplies the rated dc bias to the sample capacitor.  $R_L$  is the range resistor of the leakage current measurements. The differential amplifier has high dc gain and high input impedance, and it operates as a current-to-voltage converter. Then the bias voltage is applied through a limiting resistor  $R$  to the sample capacitor. The leakage current of this capacitor flows into the negative input terminal of the differential amplifier. But the positive input terminal is connected to ground. The potential of the negative input is forced to ground potential by its own high gain and negative feedback circuit. Therefore current through the feedback resistor  $R_L$  is equal to the leakage current  $I_L$ . Thus the leakage current can be measured by detecting the voltage drop across  $R_L$ .

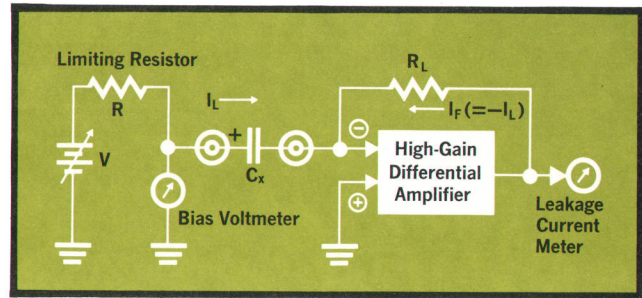


Fig. 9. Leakage current measuring circuit used in the Model 4350A.

### Acknowledgments

I wish to acknowledge the contributions of Hiroatsu Kohno who did the mechanical design and became project leader to the conclusion of this project, and of Kazunori Shibata who did the industrial design. Others associated with the project include Kuniyoshi Osada, Noriyuki Sugihara and Jun-ichi Suehiro. Thanks are also due Giichi Yokoyama, Nobuo Numasake, Art Fong and Shiro Kito for their helpful suggestions during the project.

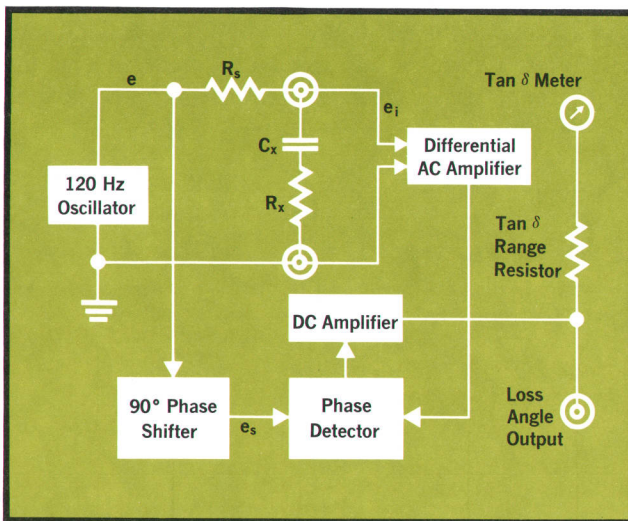
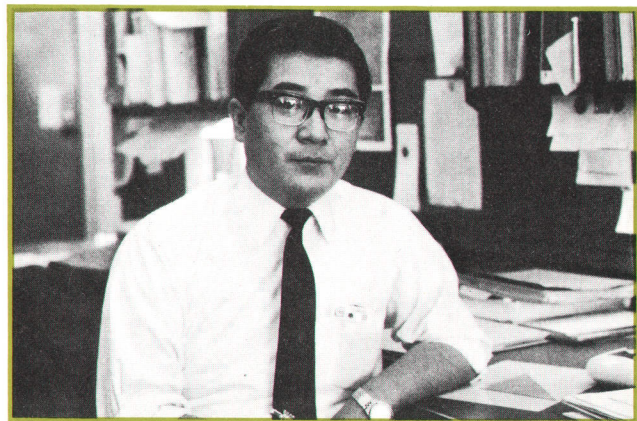


Fig. 8. Measuring circuit to determine dissipation factor.

### Outputs

The HP Model 4350A/B has two analog outputs proportional to capacitance and one proportional to loss angle. One of the capacitance outputs is 1 volt full scale for any capacitance range and the other is either 1 or 0.3 volts full scale depending upon range setting. The loss angle output is proportional to the loss angle at the rate of 0.1 volt per degree. The 1-volt capacitance output and loss angle output can be used with an analog comparator as a rapid go/no-go test system for electrolytic capacitor measurements, or with an analog recorder. The 1 or 0.3 volt capacitance output can be connected to a digital voltmeter for higher accuracy.



### Yoshihisa Kameoka

This is the second Hewlett-Packard Journal article by Yoshihisa in less than a year. His previous work discussed high and low resistance measurements (March 1971). He has been involved in design and development of instruments for measurement of component parameters at the high and low ends of the usual ranges.

Yoshihisa received his BSEE from Iwate University in 1962, then joined Yokogawa Electric Works (YEW) as a research and development engineer. He joined Yokogawa-Hewlett-Packard in 1964. He was the first project leader of this 4350A/B development.



## SPECIFICATIONS

### HP Model 4350A/B High Capacitance Meters

#### CAPACITANCE MEASUREMENT

##### CAPACITANCE

RANGE: 1  $\mu$ F to 300 mF full scale in 12 ranges in 1, 3, 10 steps.  
 MINIMUM RESOLUTION: 0.02  $\mu$ F at 1  $\mu$ F full scale.  
 ACCURACY (% of full scale):

Tan $\delta$ Range	Capacitance Range Full Scale	
	1 $\mu$ F to 100 mF	300 mF
0 to 1	$\pm 3\%$	$\pm 4\%$
1 to 5	$\pm 4\%$	$\pm 5\%$

##### TAN $\delta$

RANGE: 0.5 or 5 full scale in 2 ranges.  
 MINIMUM RESOLUTION: 0.05 at 0.5 full scale.  
 ABSOLUTE ACCURACY:

$$0.5 \text{ Full Scale: } \pm 0.025$$

$$5 \text{ Full Scale: } \pm 0.06 + \frac{(\text{reading})^2}{20}$$

$$- 0.06 + \frac{(\text{reading})^2}{25}$$

##### INTERNAL TEST SIGNAL

FREQUENCY: 120 Hz  $\pm 5$  Hz.  
 STABILITY:  $\pm 0.5\%$  0°C to 50°C.  
 VOLTAGE ACROSS UNKNOWN: 0.5 to 2.5 mV rms, depending on magnitude of tan  $\delta$ . Open circuit, typically 1V rms.

##### INTERNAL DC BIAS

VOLTAGE RANGE: 0 to 6V dc, continuously adjustable. Voltage can be monitored by internal voltmeter.  
 VOLTMETER: 10V dc full scale,  $\pm 5\%$  of full scale.  
 RESPONSE TIME (C and tan  $\delta$ ): Typically 1s.\*

##### LEAKAGE CURRENT MEASUREMENT (4350A only)

##### CURRENT

RANGE: 1  $\mu$ A to 10 mA full scale in 9 ranges in 1, 3, 10 steps.  
 MINIMUM RESOLUTION: 0.02  $\mu$ A at 1  $\mu$ A full scale.  
 ACCURACY:  $\pm 3\%$  of full scale.  
 METER PROTECTION: Meter is protected from charging surge currents.

##### DC BIAS VOLTAGE

INTERNAL: Up to 100V dc in 2 ranges, continuously adjustable.  
 EXTERNAL: 600V dc maximum.  
 VOLTMETER MONITOR  
 RANGES: 10V or 100V dc full scale for internal dc bias.  
 1000V dc full scale for external dc bias.  
 ACCURACY:  $\pm 5\%$  of full scale.

##### PROTECTION RESISTOR

Used to protect sample and internal dc source from damage by large charge currents.  
 INTERNAL: 1 k $\Omega$ .  
 EXTERNAL: Resistor may be used to reduce charge time.

##### WARNING LAMP

Indicates 'DANGER' when dc voltage across unknown is higher than 1.5V dc.

##### ANALOG OUTPUTS

CAPACITANCE OUTPUTS  
 1V dc at any full scale range: for use with analog comparator.  
 1V dc or 0.3V dc full scale: for use with DVM.

##### ACCURACY:

Tan $\delta$	Capacitance Range Full Scale	
	1 $\mu$ F to 100 mF	300 mF
0 to 1	$\pm(1.5\% \text{ of reading} + 0.5\% \text{ of full scale})$	$\pm 3\%$ of full scale
0 to 5	$\pm(1.5\% \text{ of reading} + 1.5\% \text{ of full scale})$	$\pm 4\%$ of full scale

OUTPUT IMPEDANCE: Less than 1.5 k $\Omega$ .  
 OVERRANGE: 25% of full scale.  
 RESPONSE TIME: Typically 0.5 s.\*  
 LOSS ANGLE ( $\delta$ )

Analog output voltage vs  $\delta$ : 0.1V/degree.

Tan $\delta$	$\delta$	Output voltage
0 to 0.5	0° to 26.6°	(0 to 2.66V dc) $\pm 0.13$ V dc
0.5 to 5	26.6° to 78.7°	(2.66 to 7.87V dc) $\pm 0.3$ V dc

RESIDUAL NOISE: 40 mV p-p maximum  
 RESPONSE TIME: Typically 0.6 s.\*

##### GENERAL

TEMPERATURE RANGE: 0°C to 50°C.  
 POWER: 115V or 230V  $\pm 10\%$ , 50 Hz to 400 Hz, approx. 35 W.  
 DIMENSIONS: 7-25/32 in wide, 6-17/32 in high, 12 in deep  
 (198 x 166 x 305 mm).  
 WEIGHT: Net 11 lb (4.8 kg), shipping 15 lb (6.8 kg).

##### ACCESSORIES FURNISHED

16035A test cable with four alligator clips.  
 16036A test cable with two alligator clips.  
 7-foot power cable with NEMA plug.

##### PRICE IN U.S.A.:

HP Model 4350A, \$880.  
 HP Model 4350B, \$775.

##### MANUFACTURING DIVISION:

YOKOGAWA-HEWLETT-PACKARD, LTD.  
 9-1 Takakura-cho  
 Hachioji-shi, Tokyo, Japan

\* If measurement with dc bias is required sample should be allowed to charge prior to reading.





# Measuring True RMS AC Voltages To 100 MHz

By J. B. Folsom

*Broadband measurements of true rms voltage  
used to be costly or inaccurate or both.*

UNTIL RECENTLY, GENERAL PURPOSE AC VOLTMETERS FELL INTO TWO CATEGORIES: analog instruments having midband accuracies of 1% or 2%, and digital instruments with midband accuracies of 0.1% or better. The analog instruments had the widest bandwidths and the lowest prices. Those who wanted accuracy or resolution better than about 1% were forced to use a digital instrument. The digital instruments, in general, were accurate 4- or 5-digit dc voltmeters that included ac converters. If the ac converter were one of the 'average-detecting' or quasi-rms types, errors of 1% or 2% were still probable unless the waveform happened to be a harmonically-pure sine wave (or in some instruments, one or two other specific waveforms). If the converter were a true-rms type such waveform-related errors were not present, but it was even more expensive. The initial choice was quite simple: low accuracy or high cost.

Thus the project which wound up with the HP 3403A and 3403B True-RMS Voltmeters aimed at a combination of features and capabilities previously unobtainable. The 100-MHz bandwidth target was 5 times that of even the widest band analog types (excluding, of course, the RF-only voltmeters). Midband accuracy was to be better than that realizable by anything other than very costly true-rms digital types.

As developed, the 3403A (Fig. 1) in addition to measuring true rms ac can also measure directly the rms value of a waveform containing both ac and dc, and it can measure the dc component alone; the 3403B measures true rms ac only. A dB option allows the choice of readings either in volts

or in dB; the dB reference is adjustable. Autoranging is optionally available, as are systems features (remote programming and control, and BCD outputs, isolated or not). The 3403A input connector can be floated, a common need for dc or low-frequency measurements. Input impedance is high, so any of the usual voltmeter measurements may be made. The block diagram is shown in Fig. 2.

## Input Attenuator

Although the characteristics of the input attenuator are respectable enough, they are not individually particularly unusual. What is unusual is that characteristics which tend to be mutually exclusive are achieved simultaneously. Consider this combination of characteristics:

1. DC to 100 MHz bandwidth
2. Input impedance  $10\text{ M}\Omega$  in parallel with 19 pF
3. 1000 V maximum input voltage (at any range setting)
4. Remotely programmable

Attenuators designed for frequencies up to 100 MHz are usually low impedance (e.g.  $50\Omega$ ), but such an input impedance is not compatible with the requirements of a general-purpose voltmeter, which is often used to make measurements where the source impedance may be as high as  $10^4$  or  $10^5\ \Omega$ , or where the voltage may be as high as 1 kV.

The 3403 attenuator is a typical RC design. The 100-MHz bandwidth was achieved only by paying strenuous attention to all the stray capacitances and inductances in the layout. Because of the high-voltage remotely-controlled switching required, reed switches are used.

In keeping lead lengths as short as possible to



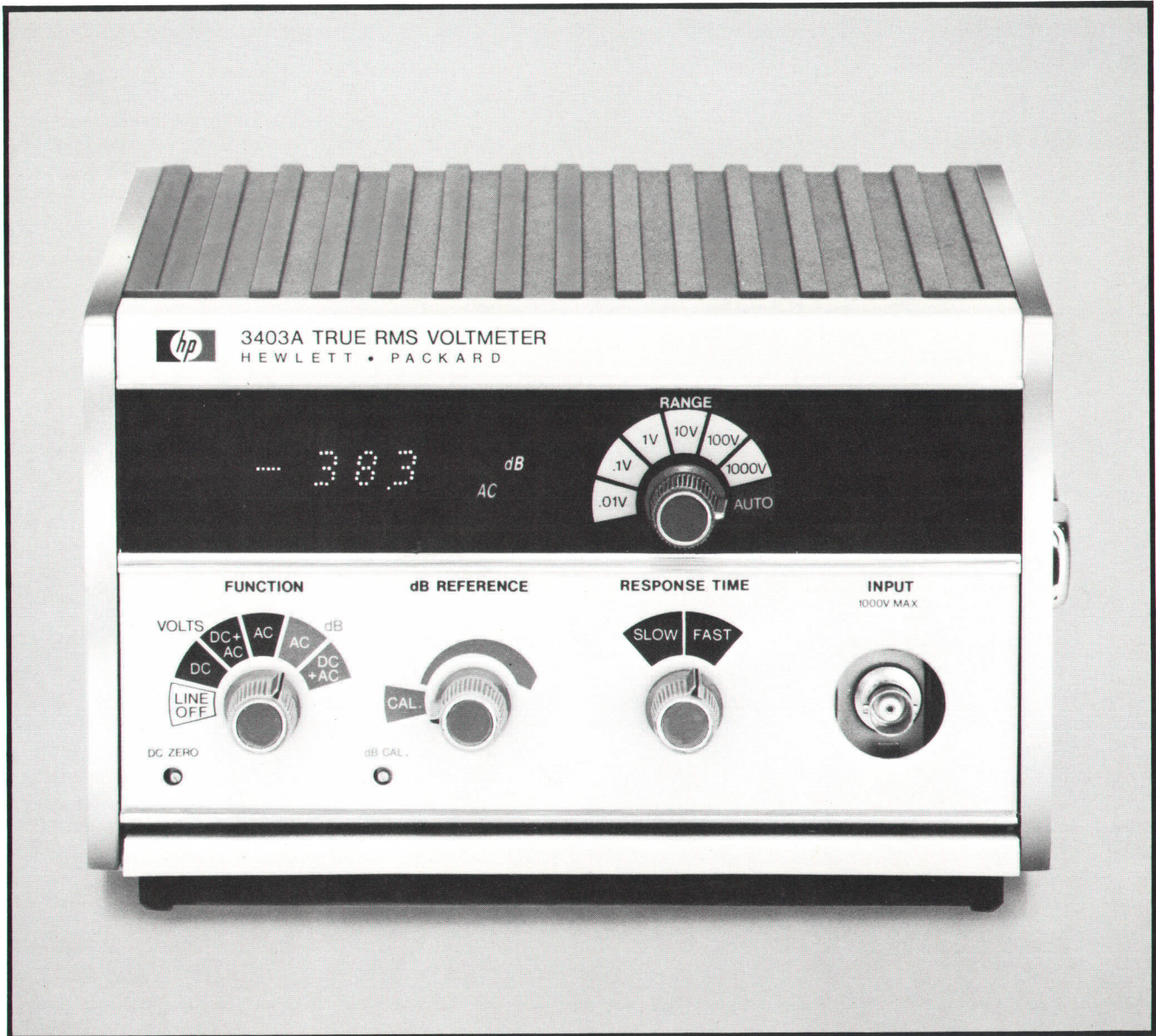


Fig. 1. Model 3403A 100-MHz true-rms Ac voltmeter.

minimize inductances (in one case the length of the reed switch itself is the limiting factor), components are placed physically close to each other, and thereby stray capacitances are made larger. The design was simplified somewhat by the fact that the full 100-MHz bandwidth isn't necessary on the high attenuation settings; the engineer who needs to measure 1 kV at 100 MHz is rare indeed! An upper limit of  $10^8$  V Hz is specified.

#### Input Connector

Even an item so apparently trivial as the input connector can present problems when a truly general-purpose input is required. For frequencies

up to 100 MHz, a coaxial connector such as BNC must be used. But the typical user at dc or audio frequencies is accustomed to using the familiar dual banana jack, and often wants to make measurements where the common is floated by as much as several hundred volts. Allowing a BNC connector to be floated at such voltages presents an unacceptable safety hazard.

The solution to this dilemma is in arranging so the input may be either BNC or floating, but not both simultaneously. A special adapter is provided which changes the grounded BNC connection to a floating dual banana jack. Attaching the adapter to the BNC input opens a microswitch



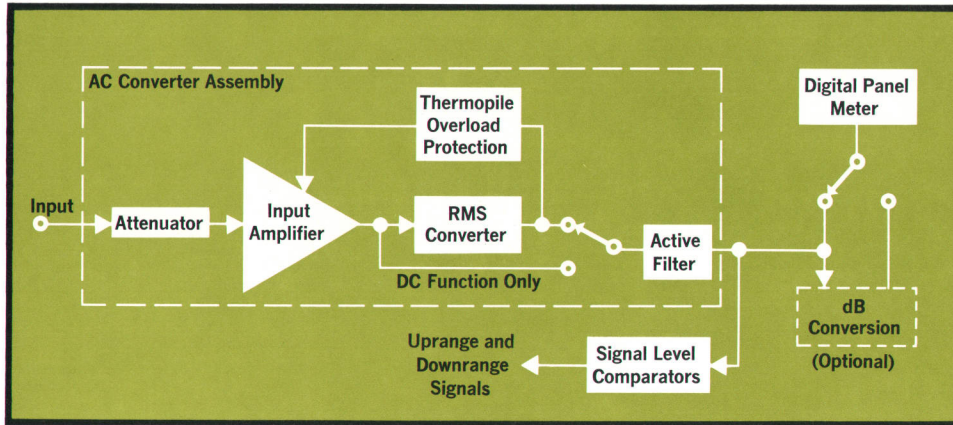


**Fig. 2.** The basic design of the 3403A is simple and straightforward. The performance of the instrument is largely due to the capabilities of the hardware used. Included are HP-built components using six different new technologies: 1) thin-film hybrid, 2) monolithic bipolar (conventional), 3) monolithic bipolar (high frequency), 4) MOS LSI monolithic, 5) thin-film vacuum thermopile, and 6) GaAsP light-emitting diodes.

which completes the ground path and therefore precludes floating when the adapter is not used.

### Input Amplifier

The input amplifier (Fig. 3), like the input attenuator, is unusual not because of any single characteristic, but because of the combination. This includes:

1. Input offset voltage temperature coefficient:  $<10 \mu\text{V}/^\circ\text{C}$
  2. Input offset current:  $<500 \rho\text{A}$ , 0 to  $75^\circ\text{C}$  (externally compensated)
  3. Open loop gain: 86 dB
  4. Power supply rejection:  $>60 \text{ dB}$
- That sounds pretty much like a respectable FET-

input op-amp until we add the final item:

5. Frequency response:  $\pm 0.5 \text{ dB}$ , dc to 100 MHz  
(Gain = 5,  $E_{\text{out}} = 0.5 \text{ V rms}$ ,  $R_L = 70\Omega$   
paralleled by 10 pF)

To accommodate a 10-mV range, the gain of the amplifier is switched from 14 dB to 34 dB by switching the feedback network on the substrate.

An interesting design problem was that of obtaining good high-frequency grounds in a plug-in package. For ease of use the dual-in-line plug-in configuration was desired, but grounding was inadequate. The solution is a metal block which serves as both ground path and heat sink. The ceramic substrate is cemented into the U-shaped

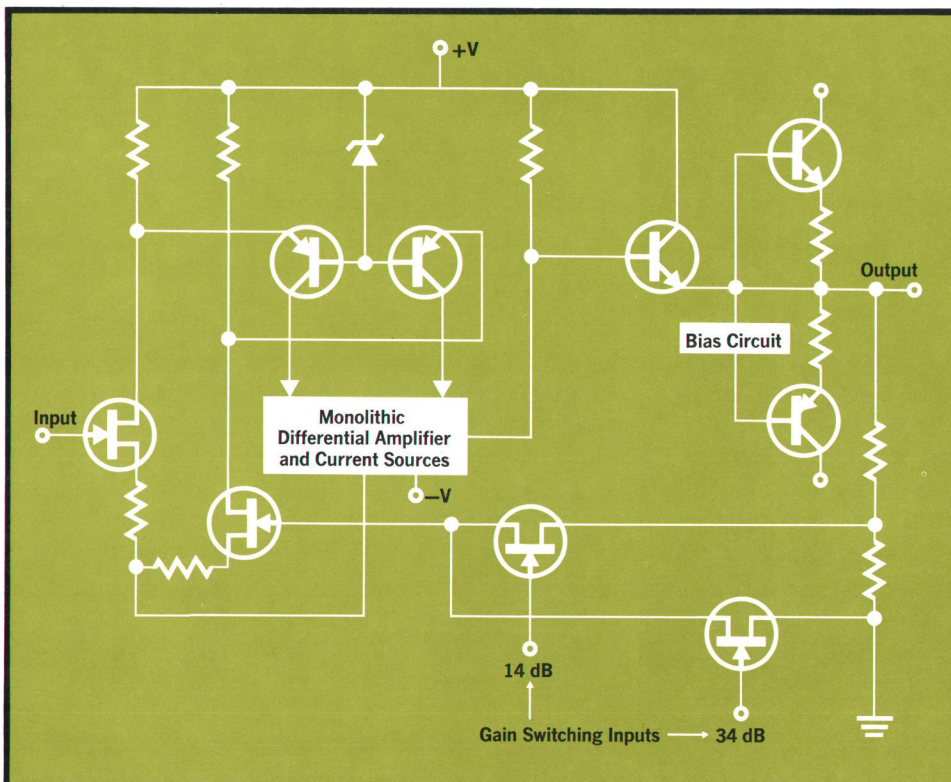


**Fig. 3.** Input amplifier simplified schematic. The 3403 input amplifier uses a combination of technologies. The substrate is ceramic with laser-trimmed thin-film resistors and conductors. Mounted on the substrate in chip form are JFET's, diodes, bipolar transistors, a high-frequency monolithic bipolar IC, MOS capacitors, and ceramic capacitors. Except for emitter-follower output drive the entire circuit is differential.



block, which is screwed directly to the hermetic aluminum casting which houses the entire ac to dc converter. The ground path is from the ceramic to the heat sink (via leads at each corner of the substrate) and from there to the casting. Thus the package is essentially a plug-in but has ground connections screwed to the casting. The heat-sink block gives some important side benefits: heat conduction to the casting is excellent and the substrate is made nearly isothermal, all of which aids in minimizing dc drift. The bathtub shape reduces the possibility of damage due to handling during fabrication by recessing the substrate.

For the 3403B, or when the 3403A is used in the ac mode, one might expect that the dc performance of the input amplifier would not matter, but this is not quite true. Because of the combination of low and high frequencies which must be handled, coupling capacitively to the amplifier load is impractical. A capacitor large enough to pass the low frequency end of the spectrum would be out of the question due to its high-frequency constraints. Therefore the amplifier must still be dc-coupled. Since any dc output heats the thermopile just as well as does ac, the dc must be well controlled even for measuring only ac. This is done by adding a high-gain low-pass feedback path around the input amplifier, so any dc at the output is fed back to the input amplifier's second stage. The dc offset at the output thus is reduced to the value of the input offset of the feedback amplifier. In addition to eliminating the effects of both the offset voltage drift and offset current drift of the input amplifier itself, the effect of any dc leakage of the input coupling capacitor is also eliminated. When measuring millivolts of ac while blocking hundreds of volts of dc, the leakage of even a good capacitor can become significant, particularly at higher temperatures.

### RMS Converter

The basic circuit of the true-rms converter (Fig. 4) is really quite simple; the departures from prior designs are made possible primarily by hardware produced by new technologies. The dual thermopile originated as a variation of the optical thermopile designed for the HP 8334A Radiant Flux Detector.<sup>1</sup>

The basic configuration was modified to use resistive rather than radiant power input. Because of the high sensitivity resulting from the multi-junction thermopile, amplifier A<sub>1</sub> could be built without using choppers. A<sub>1</sub> is a bipolar monolithic amplifier tailor-made in-house for the application; the chip also includes amplifier A<sub>2</sub>. Since A<sub>1</sub> has

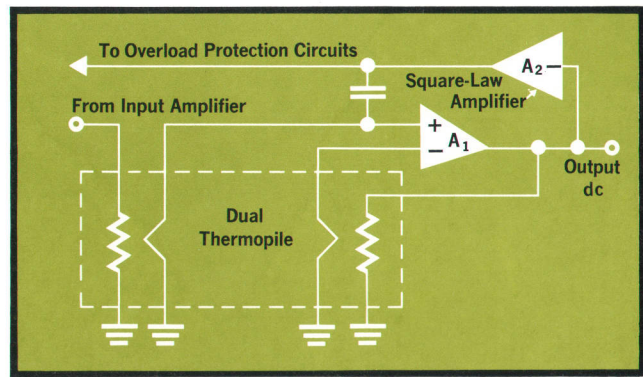


**Fig. 4.** *Trus RMS AC-DC converter. Heat produced by the signal power in the input half of the dual thermopile drives the input of amplifier A<sub>1</sub>. A<sub>1</sub> drives feedback half until the feedback signal equals the input signal; thus the output dc equals the rms (heating) value of the input signal. At low frequencies, where the thermal time constant of the input half is too short to filter the thermopile output effectively, the ac feedback path through A<sub>2</sub> provides necessary filtering.*

a square-law device (the feedback thermopile) in its feedback path, the closed loop gain of the combination of those two elements has a 'square-root-law' characteristic. If A<sub>2</sub> were a linear gain element, the ac feedback signal would also be related to the input level by the square root, with the result that the effective time constant of the circuit would be inversely proportional to the signal level. Therefore A<sub>2</sub> is made approximately square law, giving a time constant independent of level. It is interesting to note that the lower limit of frequency which the converter can handle is determined only by practical limitations on the size of the feedback capacitor. The minimum frequency of the standard 3403A is 2 Hz (1 Hz can be measured accurately if the input contains little or no dc). Special versions can be built extending the lower limit by as much as a decade.

As with conventional thermocouples, the thermopile can be easily burned out if the input element is overdriven. The output of amplifier A<sub>2</sub> is used to prevent burnout via a circuit which switches off the power supplies to the output driver stage of the input amplifier whenever the voltage generated by the input thermopile exceeds a given level.

### dB Option

With this option, the reading can be displayed either in voltage or in dB. In the dB mode, the display is normally in dBV (0 dB=1 volt). To accommodate other dB reference levels, two controls are provided, a 'dB Reference' control and a 'dB Cal' screwdriver adjustment. By turning the 'dB Ref-



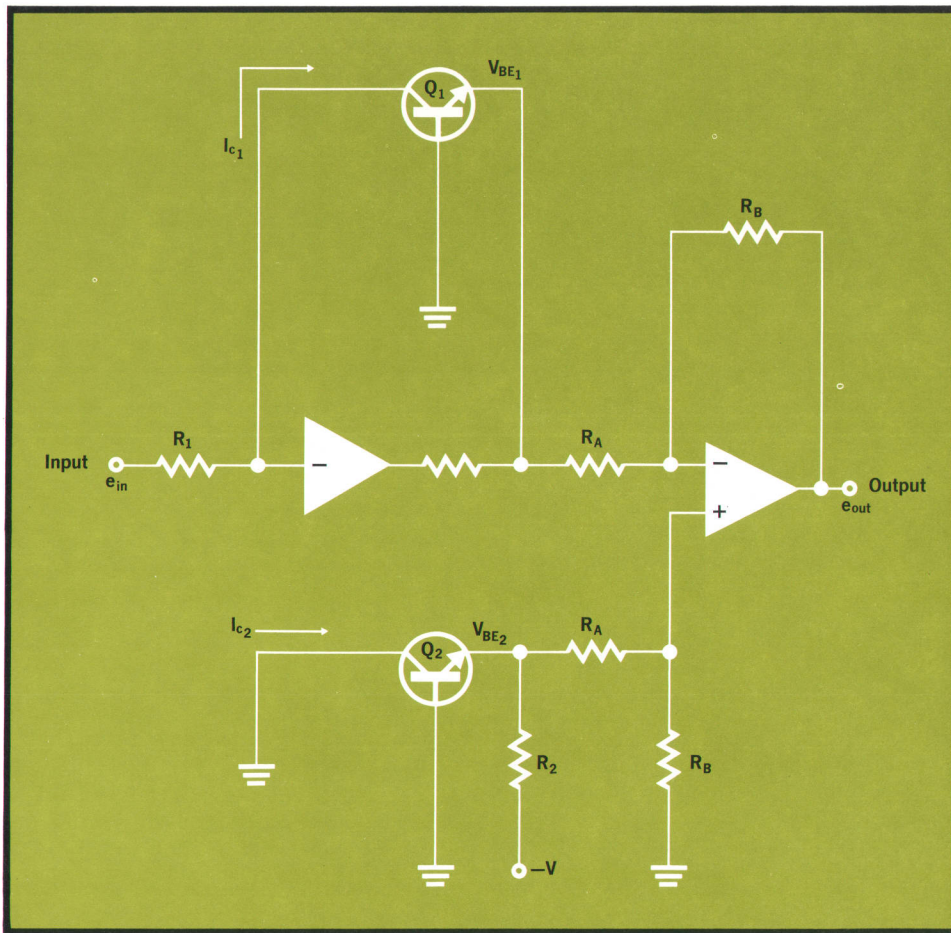


**Fig. 5.** Log Converter uses the logarithmic relationship between base-emitter voltage and collector current:

$$I_c = I_s \left( e^{\frac{qV_{BE}}{nKT}} - 1 \right).$$

For forward-biased junctions the 1 is negligible and the input to the second amplifier can be written as

$$V_{BE1} - V_{BE2} = \frac{nKT}{q} \left( \ln \frac{I_{c1}}{I_{c2}} - \ln \frac{I_{s1}}{I_{s2}} \right)$$

$$\text{Since } I_{c1} = \frac{e_{in}}{R_1}$$

$$\text{and } e_{out} = \frac{R_B}{R_A} (V_{BE1} - V_{BE2}),$$

$$e_{out} = \frac{R_B}{R_A} \frac{nKT}{q} \left( \ln \frac{e_{in}}{R_1 I_{c2}} - \ln \frac{I_{s1}}{I_{s2}} \right)$$

Transistors  $Q_1$  and  $Q_2$  are fabricated as part of a monolithic bipolar IC which includes circuitry that maintains the chip temperature at a constant value. Thus the ratio  $I_{s1}/I_{s2}$  is fixed, as is the gain constant  $nKT/q$ . The dB reference level is easily shifted by varying either  $R_1$  or  $I_{c2}$  (via  $R_2$ ).

reference' control from the detented 'Cal' position, the reference level can be shifted downward more than 10 dB. This means that any arbitrary level on any range can be made to read either 0 dB or some multiple of 10 dB. This can be very convenient when, for instance, a frequency response is measured. The 'Cal' position of this control can itself be adjusted approximately 3 dB by using the 'dB Cal' adjustment, enough to change the detented position to 0.775 V (0 dBm, 600Ω), which is a commonly used reference level. By using both controls, the 0 dB level can be set as low as 0.224 V (0 dBm, 50Ω). A simplified schematic of the dB option's Log Converter is shown in Fig. 5.

#### dB Display Ranging

As in most digital voltmeters, the basic ranging method involves changing the input attenuation or gain by factors of 10 and changing the decimal point and/or units displayed. However, when the display is to be in dB, a different scheme must be used, since a change of one range requires the display to change by 20.0 dB. Fig. 6 shows how an internally-produced digital IC, built into the Digital

Panel Meter, is used to add or subtract increments of 20 dB.

#### Mechanical Design

To as great an extent as was physically possible, each of the functional blocks was made a plug-in module or plug-in PC board. Removal of the side covers also releases the bottom cover, giving access to all the plug-ins. The power supply, for example, can be separated from the rest of the instrument and operated independently by removing two screws and unplugging its PC board edge connector; the two wires to the power switch are the only remaining tie. Safety requirements prevent these from being run through the PC boards.

#### AC Converter

The AC Converter Assembly is a completely self-contained module, comprising all those functions inside the dotted line on the block diagram. Except for the input signal itself, all the connections to this module are dc: dc output, power supplies, and programming logic lines. To prevent RFI, the attenuator, input amplifier, and thermopile were built



within a closed metallic container (Fig. 6). This container is a casting, which was expanded in size to include the entire ac-dc conversion function. The

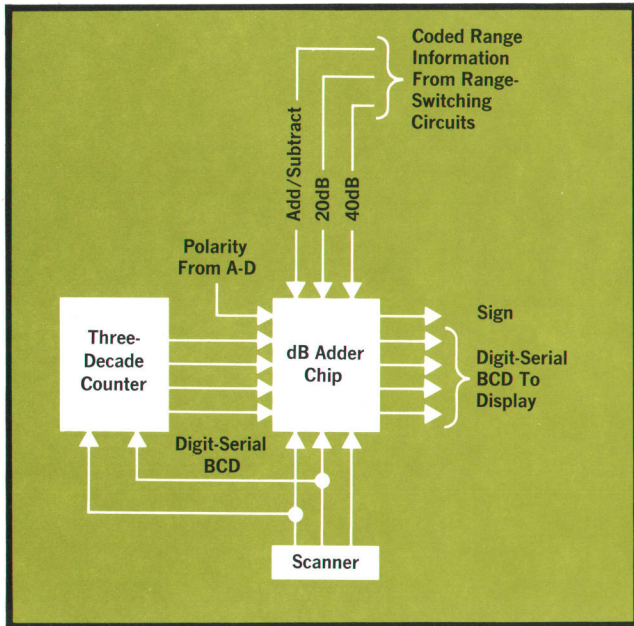


**Fig. 6.** Ranging of dB display. A single MOS chip, a serial adder, performs display ranging in the dB mode. Signals from range-switching circuits command the adder chip to add or subtract 20, 40 or 60 dB to or from the serial BCD generated by the A-D Converter of the digital panel meter.

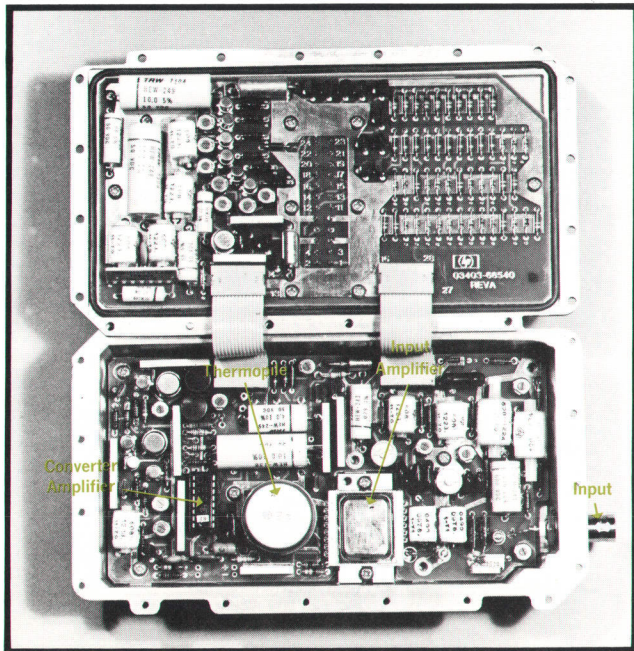


**Fig. 7.** AC converter assembly. Aluminum casting is hermetically sealed to prevent high-frequency humidity problems. Inside is the thin-film thermopile and the dc-to-100 MHz thin-film hybrid IC amplifier.

casting was designed to be hermetically sealed, eliminating the problems which normally occur in such high-impedance circuits under high-humidity conditions. From the block diagram it may be seen that this protection encompasses most of the instrument's critical analog circuits.

### Rear Input

Especially in systems applications it's desirable to have the input on the rear of the instrument. In most voltmeters this is accommodated by some special adaptation, which usually involves some cabling from the front to the rear of the instrument and some sacrifice in performance at higher frequencies. Where a high-impedance 100-MHz input is involved, such an approach is simply out of the question. The 3403 solution to this problem is unique. The ac converter assembly is symmetrical about the connector (on the back of the casting) which is its tie to the instrument's motherboard; moreover it is symmetrically located with respect to the front and rear panels. To obtain a rear input to the instrument, the AC Converter Assembly is simply unplugged from the motherboard, turned end-for-end, and replaced into the instrument. The input characteristics and the frequency response are unaffected by the change.

### Acknowledgments

While the 3403 was developed by the Hewlett-Packard Loveland Instrument Division, the devices used and the technologies involved are the result of cooperation with three other divisions: HP Labs, HPA, and Santa Clara. The project began in 1967 under the leadership of William G. (Bill) Smith. Much credit is due to those who contributed to the design effort: Paul Febvre and Gary Peterson—product design; Dennis Wilkins, Terry Tuttle, and Will Cowan—input amplifier; Al Gookin and Bob Hetzel—log converter; John Keith—autorange and remote I/O; Joe Marriott—AC Converter Assembly. Particular appreciation is extended to the members of the Loveland Integrated Circuit Department.

### References

1. Charles L. Hicks and Michael R. Mellon, 'Optical Power Measurements Made Easy,' Hewlett-Packard Journal, July 1971.





## J. B. Folsom

Jerry Folsom was the first of the engineers at HP Loveland to become involved in IC design. For the present project he did the monolithic bipolar IC's for the rms converter amplifier, the log converter, and the input amplifier. His BSEE (1955) was from the University of Utah, and he took the MSEE from the University of Southern California in 1957 on a Hughes Aircraft Company fellowship. He came to HP in 1965, and is now group leader for IC design. Colorado suits Jerry, his wife, and five youngsters, who enjoy camping and hiking together.

### SPECIFICATIONS HP Model 3403A True RMS Voltmeter

#### RANGES

FULL RANGE DISPLAY: From 10.00 mV (ac only) to 1000 V in 6 decade ranges.  
OVERRANGE: >90% on all ranges except as limited by max input voltage.

RANGING INFORMATION: Front panel annunciators indicate overrange (approx 190% of full range) or underrange (approx 17% of full range).

#### PERFORMANCE

##### AC FREQUENCY RANGE:

Slow response: 2 Hz to 100 MHz.  
Fast response: 25 Hz to 100 MHz.

RESPONSE TIME (to within  $\pm 0.1\%$  of input change):

Fast response: 1 s.  
Slow response: 10 s.

##### DISPLAY RATE:

Fast response: 4 readings per s.  
Slow response: 1 reading per s.

##### FUNCTIONS

DC: Responds to dc component of input signal.

AC: Responds to true rms value of ac-coupled input signal.

AC + DC: Responds to true rms value of dc and ac input signal; reading is

$$\sqrt{(dc)^2 + (ac_{rms})^2}$$

TEMPERATURE COEFFICIENT:  $0.1 \times$  reading accuracy/ $^{\circ}\text{C}$  outside  $25^{\circ}\text{C} \pm 5^{\circ}\text{C}$  temperature range.

READING ACCURACY (=  $\pm$  % OF RANGE  $\pm$  % OF READING) % OF RANGE

RANGE	VOLTS			FREQUENCY (Hz)					
	DC	DC+AC	AC	DC	25	100K	1M	10M	100M
1000V	.3	.3	.3	.1	.4*	.2			
100V	.2	.2	.2	.1	.4*	.2	1		
10V	.2	.2	.2	.1	.4*	.2	.5	1	
1V	.2	.2	.2	.1	.4*	.2	.5	1	2 5
100mV	.6	.6	.2	.1	.4*	.2	.5	1	2 5
10mV			.4						20M
			.4						2M

For 90 days ( $25^{\circ}\text{C} \pm 5^{\circ}\text{C}$ , <95% RH, 17% of range to 190% of range.)

CAUTION: Frequencies and ranges in this area may result in invalid readings without ranging indication.

\*dc + ac function and slow response time only.

#### INPUT CHARACTERISTICS

##### INPUT IMPEDANCE

<10MHz.

1 V to 1000 V range:  $10 \text{ M}\Omega \pm 10\%$  shunted by  $18 \text{ pF} \pm 10\%$ .

10 mV and 100 mV ranges:  $20 \text{ M}\Omega \pm 10\%$  shunted by  $14 \text{ pF} \pm 10\%$ .  
10 MHz and 100 MHz: Table gives maximum loading across terminated source.

System impedance (source and load)	Frequency	
	10 MHz	100 MHz
50 $\Omega$	1%	10%
75 $\Omega$	2%	20%

#### CREST FACTOR:

2 Hz to 200 Hz: 2:1 at full range input.  
>200 Hz: 10:1 at full range input.

#### MAXIMUM INPUT VOLTAGE:

Hi to Lo:  
1000 V rms, 1500 peak or  $10^6$  V-Hz on any range.  
Maximum dc voltage in ac mode: 500 V dc.

#### Lo to Chassis:

500 V dc, when floated with special banana-to-BNC adapter.  
NORMAL MODE REJECTION >60 Hz (DC mode): >60 dB.  
EFFECTIVE COMMON MODE REJECTION 60 Hz (with 1 k $\Omega$  unbalance in either lead):  
AC mode: >60 dB.  
DC mode: >120 dB.

#### OPTIONS

##### AUTORANGING (Option 001)

AUTOMATIC RANGING: Uprange at approx 190% of full range; downranges at approx 17% of full range.

##### AUTORANGE TIME:

Fast response: 1 s per range change.  
Slow response: 10 s per range change.

##### DIGITAL OUTPUT (Option 002)

##### OUTPUT LINES:

4 line BCD (+8421 low true),  
4 columns for measurement magnitude.  
1 column for decimal point location.  
1 column for polarity and out-of-range information.  
1 column for function.

##### INPUT LINES:

Printer Hold-off.

##### Measure.

##### REMOTE CONTROL + DIGITAL OUTPUT + AUTORANGING (Option 003)

Provides all features of Digital Output and Autoranging plus remote programming of all front panel functions.

##### ISOLATED DIGITAL OUTPUT (Option 004)

In addition to the features of Option 002, provides isolation between measurement input terminals and digital output lines.

##### ISOLATED REMOTE CONTROL + DIGITAL OUTPUT + AUTORANGING (Option 005)

Combines features of Options 003 and 004.

##### dB DISPLAY (Option 006)

MEASUREMENT RANGE: 103 dB ( $-48 \text{ dB V}$  to  $+60 \text{ dB V}$ ).  
CALIBRATED dB REFERENCE: 0 dB = 1.000 V; reference level may be set for 0 dBm (600 $\Omega$ ) by adjusting front panel dB calibration adjustment.

VARIABLE dB REFERENCE: Reference level may be shifted downward from calibrated position by >13 dB.

##### dB RECORDER OUTPUT:

Output Voltage: 200 mV for 20 dB.  
Output Resistance: 1 k $\Omega \pm 500 \Omega$ .

### HP Model 3403B True RMS Voltmeter

Specifications are identical to those of Model 3403A with following exceptions:

AC FREQUENCY RANGE: 25 Hz to 100 MHz except 10 mV range.  
10 mV range: 50 Hz min.

RESPONSE TIME: 1 s.

FUNCTIONS: AC volts, ac db (optional).

INPUT: BNC grounded to chassis—non-floating.

##### OPTIONS:

Digital Output (Option 002)

dB Display (Option 006)

##### GENERAL (both models)

##### OPERATING CONDITIONS:

Temperature Range:  $0^{\circ}\text{C}$  to  $50^{\circ}\text{C}$ .

Humidity: <95% RH.

##### RECORDER OUTPUT:

Output Voltage: 1 V dc open circuit for full range input.

Output Resistance: 1 k $\Omega \pm 10\%$ .

POWER: 115 V or 230 V  $\pm 10\%$ , 48 Hz to 440 Hz, 35 VA maximum (including all options).

INPUT TERMINALS: BNC front-panel connector standard for Lo and Hi terminals; rear panel connector available by internally reversing position of AC Converter Module.

DIMENSIONS: 7 3/4 in wide x 5 in high x 9 1/4 in deep (197 x 127 x 235 mm).

WEIGHT (including all options): Net, 11 lb (5 kg); shipping, 12 lb (5.5 kg).

##### PRICE in U.S.A.:

HP 3403A	\$1400
Option 001 AUTORANGING	\$125
Option 002 DIGITAL OUTPUT	\$150
Option 003 REMOTE CONTROL + DIGITAL OUTPUT + AUTORANGING	\$290
*Option 004 ISOLATED DIGITAL OUTPUT	\$290
*Option 005 ISOLATED REMOTE CONTROL + DIGITAL OUTPUT + AUTORANGING	\$450
*Option 006 db DISPLAY	\$250
*Option 004, 005, 006 are available only as factory-installed options.	
HP 3403B	\$1150
Option 002 DIGITAL OUTPUT	\$150
Option 006 db DISPLAY	\$250
MANUFACTURING DIVISION: LOVELAND DIVISION	
815 Fourteenth Street, S.W.	
Loveland, Colorado 80537	

HEWLETT-PACKARD JOURNAL



MARCH 1972 Volume 23 • Number 7

Technical Information from the Laboratories of Hewlett-Packard Company, 1501 Page Mill Road, Palo Alto, California 94304 U.S.A.  
Hewlett-Packard S.A. 1217 Meyrin—Geneva, Switzerland • Yokogawa-Hewlett-Packard Ltd., Shibuya-Ku, Tokyo 151 Japan

Editor: R. H. Snyder Editorial Staff: R. P. Dolan, H. L. Roberts, L. D. Shergalis Art Director: Arvid A. Danielson Assistant: Erica R. Helstrom